

M. N. Berberan-Santos

Centro de Química-Física Molecular - Instituto Superior Técnico - P-1096 - Lisboa Codex - Portugal

Recebido em 17/9/93; cópia revisada em 3/5/94

The free-electron molecular orbital method is reviewed and generalized, in order to be applicable to the C<sub>60</sub> molecule. The model predicts two strong bands in the violet and near-UV. Comparison with experiment shows rough agreement. Discussion of the differences allows a deeper analysis of the electronic states and transitions in the singlet manifold of C<sub>60</sub>.

Keywords: free-electron molecular orbital method; C<sub>60</sub> molecule.

## 1. INTRODUCTION

The Free-Electron Molecular Orbital (FEMO) method is the simplest quantum-mechanical method for the approximate calculation of molecular orbitals (MO's), orbital energies (OE's), transition probabilities and transition energies of  $\pi$  electron systems of conjugated hydrocarbons. In spite of its crudeness, nearly quantitative results are obtained in some cases: the application of the FEMO method to symmetrical cyanine dyes, carried out in the late 40's<sup>1</sup>, is now present in most Physical Chemistry textbooks [e.g. ref. 2, pp. 424 and 533 and ref. 3, pp.440], and articles on the subject continue to appear<sup>4-6</sup>.

The availability of much more powerful methods, and respective softwares, makes the FEMO method inadequate for quantitative purposes. Nevertheless, it is of pedagogical importance, at least for three reasons: 1) It allows a meaningful (though admittedly crude) application of simple quantum models to real molecules 2) It captures essential features of the physical system with a minimum of theoretical elaboration. 3) It provides good ground for the discussion of more advanced treatments.

In this work, and after a brief review of the FEMO method in connection with the quantum models used thus far, C<sub>60</sub> electronic absorption spectrum is estimated on its basis by the use of a third quantum model (particle-on-the-sphere). Comparison with experiment shows rough agreement. Existing discrepancies are then discussed qualitatively.

## 2. THE FREE-ELECTRON MOLECULAR ORBITAL METHOD

Regardless of the specific quantum-mechanical model used, there are some general assumptions that characterize this method. They are:

- Only  $\pi$  electrons are considered
- The potential energy of the electrons is constant within a certain region of space, and infinite outside it.
- Electron-electron interaction is crudely handled by its inclusion in the constant potential mentioned in b)
- Electron spin is taken into account only through the Pauli exclusion principle

These assumptions have varying degrees of severity. They may or may not be acceptable, depending on the molecule considered.

Assumption (a) follows from the  $\sigma$ - $\pi$  separability, a highly effective empirical approximation that usually holds, even in three-dimensions<sup>7,8</sup>. Naturally, the neglect of  $\sigma$  electrons precludes the possibility of describing high-energy transitions

where these electrons participate.

Assumption (b) is the main reason for the simplicity of the FEMO method. To obtain sensible results, care is required in the selection of the region of space where electrons are "allowed". This choice, in turn, immediately determines what quantum model applies. The constant value of the potential energy in the region where the electrons exist is usually taken to be zero, hence the "free" in the method's name. But this term is unfortunate, as the constant, intrinsically negative (electrons are bound), contains both the nuclear attractive forces and the inter-electronic repulsive forces (in a very crude way). Because a change of the value of this constant merely shifts all the energy levels by the same amount and does not affect energy differences, there is the common assumption that the electron is free of interactions of any kind, except at and beyond the "walls". This makes however one to believe that the model is more unrealistic than it really is: Interactions are in fact taken into account, though through an average potential energy. In this sense, the word "free" is certainly inappropriate. On the other hand, one may regard it as an indication that the electron is fully delocalized, that is, unattached to specific nuclei or bonds. Comments similar to the above have been made by Pilar regarding the common interpretation of the Hückel Molecular Orbital (HMO) method [ref. 9, p.457]. One should add that limited freedom was in any case already implied, because the use of infinitely high barriers confines the electrons to the constant potential region regardless of the value of their energy: Ionization is not a feature of the model.

Assumption (c) is usually a severe one. The simple orbital filling according to Hund's rule, and subsequent calculation of transitions as pure one-electron excitations neglects electron correlation, approximately handled by configuration interaction (CI) in higher methods such as CNDO/S and PPP [9]. It is known that the lowest excited state is often the less affected by CI, and therefore it is for this transition, regarded as HOMO  $\rightarrow$  LUMO, that the FEMO approximation gives the best results. However, if the excited configuration resulting from the promotion of an electron from the HOMO to the LUMO yields several excited states, these will split as a consequence of CI and the one-electron excitation will be a poor approximation for the real situation<sup>10,11</sup>. We will see that this is the case for C<sub>60</sub>.

Finally, assumption (d) means that for molecules with an even number of electrons, where only singlet and triplet states are usually relevant, the computed transition energy by the FEMO method will be also in terms of a center-of-gravity between singlet  $\leftarrow$  singlet and triplet  $\leftarrow$  singlet transitions. As the result is usually compared with the value of the

singlet  $\leftarrow$  singlet transition (the triplet  $\leftarrow$  singlet being highly forbidden in hydrocarbons) reasonable results are expected only when the singlet-triplet splitting is small. It is known that for large conjugated systems this splitting is indeed small<sup>†</sup> [ref. 12, ch.3].

### 3. QUANTUM MODELS USED WITH THE FEMO METHOD

The quantum-mechanical models used with the FEMO method have been essentially of two kinds: particle-in-a-box (PIB), usually one-dimensional; and particle-on-a-ring (POR). In addition, a third model will be used in this work: that of the particle-on-a-sphere (POS).

These three well-known quantum models are discussed in most textbooks of Physical and Quantum Chemistry. They are summarized in Table I.

The one-dimensional version of the PIB model has been used to describe the all-trans symmetrical cyanine dyes<sup>1</sup>, as these are formed by a long, zig-zag conjugated chain of nearly uniform bond length, which is essentially one-dimensional. For these molecules, the FEMO method accounts well for the general absorption pattern, including relative intensities<sup>1</sup>. The POR model was used to describe the catacondensed aromatic hydrocarbons<sup>1</sup>, a class of compounds that includes benzene, naphthalene and anthracene, and for which it is always possible to define a molecular perimeter by drawing a closed line through all carbon atoms. In the FEMO method, it is assumed that  $\pi$  electrons are confined to this closed path, for simplicity taken to be circular, and along which the potential energy is

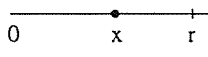
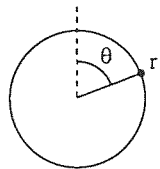
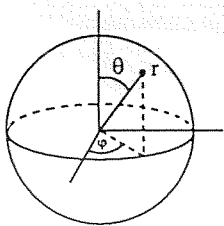
constant. The common  $L_a$ ,  $L_b$ ,  $B_a$ ,  $B_b$  state notation used for catacondensed hydrocarbons and derivatives results from the FEMO method<sup>1</sup>.

### 4. THE $C_{60}$ MOLECULE IN THE FEMO MODEL

The  $C_{60}$  molecule, Fig. 1 (fullerene-60, footballene, soccerballene, buckminsterfullerene) closely resembles a hollow sphere of 7.0 Å in diameter<sup>13</sup>. It belongs however to the truncated icosahedral point group ( $I_h$ )<sup>13</sup>, and not to the group of the sphere ( $K_h$ ). The  $I_h$  symmetry is for example made evident by the IR absorption spectrum, where in spite of the 174 normal modes of vibration, only 4 distinct intense bands appear<sup>14</sup>. For the same reason,  $C_{60}$  is the only aromatic molecule known to have intrinsically unpolarized fluorescence<sup>15</sup>. The  $\pi$ -electron cloud, comprising 60 electrons, spreads above and below the carbon skeleton.

The simplest quantum model to be used in the FEMO method is in this case that of the particle-on-the-sphere. This certainly oversimplifies the situation, as  $\pi$ -electrons are confined to a net of bonds formed by 12 pentagonal and 20 hexagonal rings and are thus not uniformly distributed over the surface as the model admits, and also because they occupy two concentric spherical shells, as mentioned, do not lying therefore on a two-dimensional spherical surface. Even so, some reasonable results are obtainable with these crude assumptions, as will be seen. The orbital energy level diagram for  $C_{60}$  and also the respective orbital filling are shown in Figure 2, the symmetry of the POS MO's being that of the spherical harmonics [ref. 2, p. 336].

Table I

QUANTUM MODEL	COORDINATES	WAVE FUNCTIONS	ENERGY LEVELS	SELECTION RULES
Particle in a one-dimensional Box		$\psi_j(x) = \sqrt{\frac{2}{r}} \sin\left(\frac{j\pi x}{r}\right)$	$E_j = \frac{j^2 h^2}{8mr^2}$  degeneracy: 1	$\Delta j = \pm 1, \pm 3, \dots$
Particle on a ring		$\Psi_{j,m_j}(\theta) = \frac{1}{\sqrt{2\pi}} e^{im_j\theta}$	$E_{j,m_j} = \frac{j^2 h^2}{2mr^2}$  degeneracy: 1 (j=0) 2 (j>0)	$\Delta j = \pm 1$ $\Delta m_j = \pm 1$
Particle on a sphere		$\Psi_{j,m_j}(\theta, \phi) = Y_{j,m_j}(\theta, \phi)$ (spherical harmonics)	$E_{j,m_j} = \frac{j(j+1) h^2}{8\pi^2 mr^2}$  degeneracy: 2j+1	$\Delta j = \pm 1$ $\Delta m_j = 0, \pm 1$

<sup>†</sup> For  $C_{60}$ , the  $S_1$ - $T_1$  splitting was experimentally estimated<sup>19</sup> as 0.30 eV.

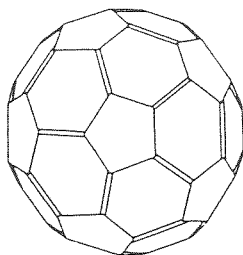


Figure 1.  $C_{60}$  showing the principal Kekulé structure.

The ground configuration of  $C_{60}$  is therefore written as  $s^2 p^6 d^{10} f^{14} g^{18} h^{10}$ . Note that the HOMO and the LUMO are both of the h type and hence of the same energy. From the selection rules given in Table 1 (POS model) both  $j=6 \leftarrow j=5$  and  $j=5 \leftarrow j=4$  one-electron excitations are allowed. These give rise to the excited configurations  $s^2 p^6 d^{10} f^{14} g^{18} h^9 i^1$  and  $s^2 p^6 d^{10} f^{14} g^{17} h^{11}$  respectively. The wavelengths associated with these transitions are readily computed from the energy level formula given in Table I and are  $\lambda(6 \leftarrow 5) = 332$  nm and  $\lambda(5 \leftarrow 4) = 399$  nm. The intensity of these transitions can also be computed, the square of the transition moment for the transition  $j+1 \leftarrow j$  being in the POS model [ref. 1, p. 479]

$$|\mu_{j+1,j}|^2 = \mu^2 \frac{j+1}{2j+1} \quad (1)$$

where in this case the equivalent permanent dipole is simply  $\mu = er$ ,  $r$  being the radius of the sphere. From this relation, transition moments of 12.6-12.7 Debye are obtained. Calculation of the oscillator strength  $f$  by the equation [ref. 2, p. 504]

$$f = \frac{8\pi^2 m_e \nu}{3h e^2} |\mu|^2 \quad (2)$$

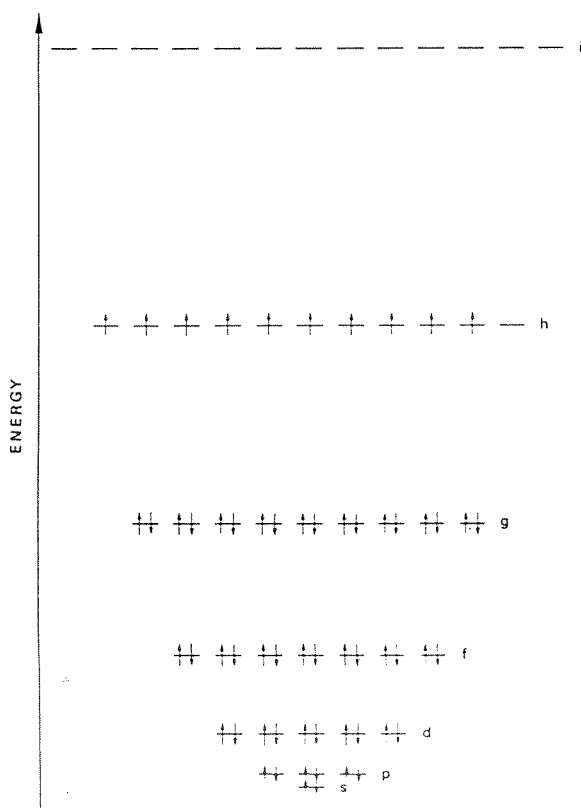


Figure 2. FEMO energy level diagram for  $C_{60}$ .

yields

$$f_{j+1,j} = \frac{2(j+1)^2}{3(2j+1)} \quad (3)$$

Computation of the numerical values gives oscillator strengths of 2.2 and 1.9, respectively, and the transitions are therefore intense.

It is perhaps remarkable that the POS model predicts here strong transitions in the violet and near UV, whereas in its usual application to linear molecules (within the rigid rotor approximation) it predicts very weak transitions in the micro-waves. The reason for the difference is mainly due to the substitution of the electron mass for the molecular reduced mass. Since the ratio of these is typically  $\sim 10^{-5}$ , and energy is inversely proportional to the mass (see Table I), energy differences increase by about  $10^5$ , hence the leap from micro-waves ( $\sim 1$   $\text{cm}^{-1}$ ) to the UV ( $\sim 10^5$   $\text{cm}^{-1}$ ). On the other hand, the oscillator strength, being proportional to the frequency, eq.2, also increases by the same factor,  $\sim 10^5$ .

Straightforward application of the FEMO method thus leads to the prediction of two strong bands somewhere in the violet and near-UV. Given the unsophisticated nature of the calculation, this is about all that can be said. In particular, the numerical values of the wavelengths, as given above, are - apart from all other approximations - strongly dependent on the radius of the sphere: A variation of 0.05 Å in  $r$  entrains a variation of ca. 10 nm in  $\lambda$ . One may incidentally make the remark that it is because of this sensitivity on interatomic distances and angles that rotational spectroscopy gives as accurate a molecular structure.

## 5. THE ELECTRONIC ABSORPTION SPECTRUM OF $C_{60}$

It is now appropriate to compare the results of the model with the published spectrum<sup>14,16-19</sup>, Fig. 3.

The (one-photon) electronic absorption spectrum of  $C_{60}$  in hexane at room temperature shows three strong bands in the near-UV at 211 nm ( $1.35 \times 10^5$   $\text{M}^{-1} \text{cm}^{-1}$ ), 256 nm ( $1.75 \times 10^5$   $\text{M}^{-1} \text{cm}^{-1}$ ) and 328 nm ( $5.1 \times 10^4$   $\text{M}^{-1} \text{cm}^{-1}$ ). These are probably 0-0 transitions, indicating similar geometries for the ground and excited (Franck-Condon) states. Any of these bands is however complex, showing several shoulders on both sides<sup>19</sup>. A sharp, weak band is observed at 406 nm. A region of very weak ( $\epsilon < 750$   $\text{M}^{-1} \text{cm}^{-1}$ ) but continuous absorption is also observed in the range 430-650 nm, 650 nm corresponding approximately to the true origin of the absorption, as shown by the study of  $C_{60}$  fluorescence<sup>20-22</sup>. This region was not expected from the

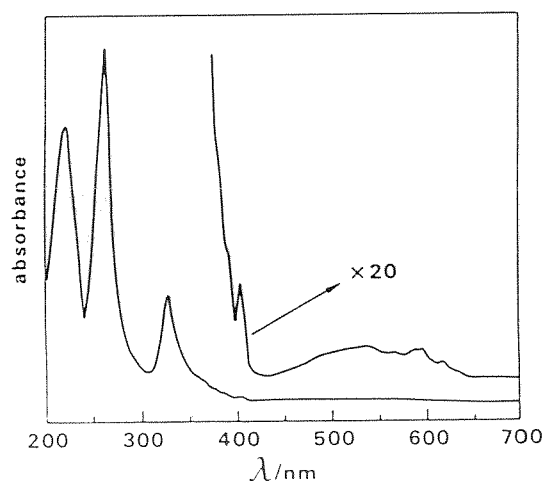


Figure 3. Electronic absorption spectrum of dilute  $C_{60}$  in cyclohexane. The solution has a magenta colour.

FEMO method. Another perturbing result that follows from the FEMO approximation is the prediction of strong paramagnetism for  $C_{60}$ , as it would possess 10 unpaired electrons (recall that there were 11 h orbitals at the HOMO level, and only 10 electrons that, according to Hund's rule would not pair, yielding the state  ${}^1H_{10}$ ).

These discrepancies can be traced back to the unrealistic assumption of spherical symmetry, when it is known that the molecule belongs to the  $I_h$  group.

Indeed, the symmetry descent from  $K_h$  to  $I_h$  produces a partial splitting of the degenerate orbitals analogous to the familiar splitting of d orbitals that occurs in inorganic complexes. The symmetry species spanned by the irreducible representations of the sphere are readily obtained from group theory<sup>23</sup> to be

$$S \rightarrow A_g \quad (4a)$$

$$P \rightarrow T_{1u} \quad (4b)$$

$$D \rightarrow H_g \quad (4c)$$

$$F \rightarrow T_{2u} + G_u \quad (4d)$$

$$G \rightarrow G_g + H_g \quad (4e)$$

$$H \rightarrow T_{1u} + T_{2u} + H_u \quad (4f)$$

$$I \rightarrow A_g + T_{1g} + G_g + H_g \quad (4g)$$

Group theory cannot be used to predict the energies of the orbitals that result, but the relative order of the orbitals can be established on the basis of calculations by the HMO method<sup>24-27</sup>. The result is shown in Fig. 4.

The ground state is now correctly predicted to be singlet. Also, as a consequence of the splitting there is an energy gap between HOMO and LUMO and thus new but forbidden ( $\Delta j = 0$  in  $K_h$ ;  $u \leftarrow u$  in  $I_h$ ) bands at low energies become possible: Owing to the still high degeneracy of most orbitals, there are several states for the same excited configuration. This means that the promotion of one electron from the HOMO to the LUMO (HOMO  $\rightarrow$  LUMO), giving rise to the excited configuration  $1a_g^2 1t_{1u}^6 1h_g^{10} 1t_{2u}^6 1g_u^8 1g_g^8 2h_g^{10} 1h_u^9 2t_{1u}^1$ , or  $2h_g^{10} 1h_u^9 2t_{1u}^1$  for short, yields the states spanned by the direct product  $H_u \otimes T_{1u}$ , that is

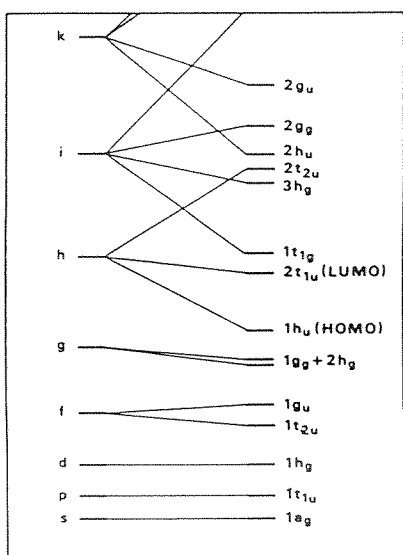


Figure 4. Orbital energy level diagram for  $C_{60}$  after the symmetry descent  $K_h \rightarrow I_h$ .

$$H_u \otimes T_{1u} = T_{1g} + T_{2g} + G_g + H_g \quad (5)$$

These transitions may become weakly allowed, however, by coupling with nearby strong ones through non-totally symmetric vibrations of adequate symmetry (Herzberg-Teller scheme). This is indeed observed<sup>18,19,22</sup>.

These four gerade states are responsible for the absorption between 550 nm and 650 nm, the lowest ( $S_1$ ) being that of  $T_{1g}$  symmetry<sup>19,22</sup>.

Given the energetic proximity between the orbital  $1t_{1g}$  (LUMO + 1) and the LUMO, the next excited configuration is  $2h_g^{10} 1h_u^9 1t_{1g}^1$ .

The states now obtained are

$$H_u \otimes T_{1g} = T_{1u} + T_{2u} + G_u + H_u \quad (6)$$

transition to one of them from the ground state being now allowed. This  $T_{1u}$  state should be the one to which the lowest allowed transition (probably at 408 nm<sup>19</sup>) occurs. The other three states probably lie at lower energies<sup>19</sup> thus contributing also to the weak absorption in the visible. In order to qualitatively discuss higher absorptions other configurations must be considered, namely those shown in Figure 5.

In doing so, one finds that  $2h_g^9 1h_u^{10} 2t_{1u}^1$  (HOMO-1  $\rightarrow$  LUMO) and  $2h_g^{10} 1h_u^9 3h_g^1$  (HOMO  $\rightarrow$  LUMO+2) are the next excited configurations that span  $T_{1u}$  states,

$$H_g \otimes T_{1u} = T_{1u} + T_{2u} + G_u + H_u \quad (7)$$

$$H_u \otimes H_g = A_u + T_{1u} + T_{2u} + 2G_u + 2H_u \quad (8)$$

and thus two other allowed transitions become possible. These two states, along with the previously identified one, should be responsible for three lowest allowed bands of  $C_{60}$  observed in the violet and near-UV, assigned at 408 nm, 377 nm and 328 nm<sup>19</sup>. The relative weakness of the 408 nm and 377 nm bands is partly attributable to the borrowed intensity by the low-lying forbidden transitions. However, a quantitative account of the spectrum can only be obtained by considering many other configurations (as many as 900 have been used<sup>19</sup>) followed by their "mixing" by the configuration interaction technique<sup>9-11,28</sup>. When this is done, any excited state becomes a superposition of configurations, and correspondence between these and absorption bands becomes more diffuse, as only relative amounts have meaning. We thus rephrase the previous discussion in terms of expected dominant contribution of a certain configuration for a given state. With this caveat, we may now try to find if the actual transitions are still traceable to the crude one-electron excitations of the FEMO model. According to Figure 5, it turns out that this is to some extent possible. The correspondence (or lack of it) may be summarized as follows:

- 1) *Weak absorption in the visible* - partly due (red-edge) to the HOMO-LUMO transition, inexistent (but forbidden)

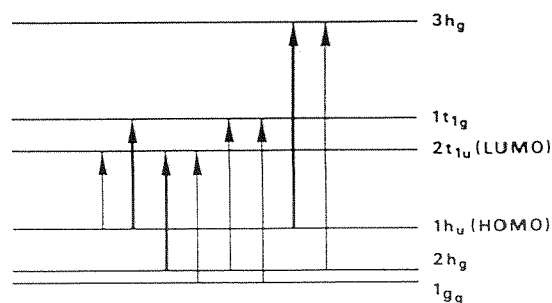


Figure 5. One-electron excitations necessary to account for the low-energy part of the absorption spectrum of  $C_{60}$ .

in the FEMO model because HOMO and LUMO are predicted to have the same energy; and partly due to the  $6 \leftarrow 5$  and  $5 \leftarrow 4$  transitions of the FEMO model.

2) *strong absorption in the violet and near - UV* - the three lowest allowed transitions (to  $T_{1u}$  states) may be associated with the  $6 \leftarrow 5$  (split into two) and  $5 \leftarrow 4$  transitions of the FEMO model, certainly mixed by configuration interaction. Higher transitions will correlate also with other excitations (e.g.  $7 \leftarrow 5$ ) forbidden in the FEMO model.

The probable order of the low-lying states is shown in Figure 6, drawn on the basis of recent studies<sup>19,21,22</sup>.

## 6. CONCLUSIONS

In spite of the fact that  $C_{60}$  was first observed eight years ago, and routinely obtained in macroscopic amounts since 1990, only the main features of its quite complex electronic absorption spectrum are understood to the present date. Available theoretical calculations account quantitatively only for the gross features<sup>25,29,30</sup> and band assignments are still incomplete. For example, the first  $T_{1u}$  band was recently placed at 408 nm<sup>19</sup>, but 328 nm is other possibility<sup>14,19</sup>. Much work remains to be done to fully unravel the detailed pattern of the electronic absorption of  $C_{60}$ . In this work, a very simple and crude model was used to gain some understanding of the

electronic absorption of  $C_{60}$ , and to motivate the discussion of more sophisticated approaches.

## ACKNOWLEDGMENTS

This work is part of the project STRDA/C/CEN/421/92 supported by JNICT (Junta Nacional de Investigação Científica e Tecnológica) and FEDER (Fundo Europeu para o Desenvolvimento Regional).

## REFERENCES

1. Bayliss, N. S.; *Quart. Rev.* (1952), 6, 319.
2. Atkins, P. W.; *Physical Chemistry*; Oxford University Press: Oxford 4th edition, (1990).
3. Shoemaker, D. P.; Garland, C. W.; Nibler, J. W.; *Experiments in Physical Chemistry*; McGraw-Hill: New York, 5th edition, (1989).
4. Farrel, J.; *J. Chem. Educ.* (1985), 62, 351.
5. Moog, R. S.; *J. Chem. Educ.* (1991), 68, 506.
6. Taubmann, G.; *J. Chem. Educ.* (1992), 69, 96.
7. Stone, A. J.; Wales, D. J.; *Chem. Phys. Lett.* (1986), 128, 501.
8. Haddon, R. C.; *Acc. Chem. Res.* (1988), 21, 243.
9. Pilar, F. L.; *Elementary Quantum Chemistry*; McGraw-Hill: New York, 2nd edition, 1990.
10. Platt, J. R.; *J. Chem. Phys.* (1950), 18, 1168.
11. Jaffé, H. H.; Beveridge, D. L.; Orchin, M.; *J. Chem. Educ.* (1967), 44, 383.
12. McGlynn, S. P.; Azumi, T.; Kinoshita, M.; *Molecular Spectroscopy of the Triplet State*, Prentice-Hall, Englewood Cliffs, N. J., 1969.
13. a) Diederich, F.; Whetten, R. L.; *Angew. Chem. Int. Ed. Engl.* (1991), 30, 678; b) Boo, W. O. J.; *J. Chem. Educ.* (1992), 69, 605.
14. Krätschmer, W.; Lamb, L. D.; Fostiropoulos, K.; Huffman, D. R.; *Nature* (1990), 347, 354.
15. Berberan-Santos, M. N.; Valeur, B.; *J. Chem. Soc. Faraday Trans.*, submitted.
16. Ajie, H.; Alvarez, M. M.; Anz, S. J.; Beck R. D.; Diederich, F.; Fostiropoulos, K.; Huffman, D. R.; Krätschmer, W.; Rubin, Y.; Schriver, K. E.; Sensherma, D.; Whetten, R. L.; *J. Phys. Chem.*, (1990), 94, 8630.
17. Hare, J. P.; Kroto, H. W.; Taylor, R.; *Chem. Phys. Lett.* (1991), 177, 394.
18. Reber, C.; Yee, L.; McKiernan, J.; Zink, J. I.; Williams R. S.; Tong, W. M.; Ohlberg, D. A. A.; Whetten, R. L.; Diederich, F.; *J. Phys. Chem.* (1991), 95, 2127.
19. Leach, S.; Vervloet, M.; Desprès, A.; Bréheret, E.; Hare J. P.; Dennis, T. J.; Kroto, H. W.; Taylor, R.; Walton, D. R. M.; *Chem. Phys.* (1992), 160, 451.
20. Kim, D.; Lee, M.; Suh, Y. O.; Kim, S. K.; *J. Am. Chem. Soc.*, (1992), 114, 4429.
21. Wang, Y.; *J. Phys. Chem.*, (1992), 96, 764.
22. Negri, F.; Orlandi, G.; Zerbetto, F.; *J. Chem. Phys.* (1992), 97, 6496.
23. Dekock, R. L.; Kromminga, A. J.; Zwier, T. S.; *J. Chem. Educ.* (1979), 56, 510.
24. Haymet, A. D. J.; *Chem. Phys. Lett.* (1985), 122, 421.
25. Haddon, R. C.; Brus, L. E.; Raghavachari, K.; *Chem. Phys. Lett.* (1986), 125, 459.
26. Fowler, P. W.; Woolrich, J.; *Chem. Phys. Lett.* (1986), 127, 78.
27. Fowler, P. W.; Lazzeretti, P.; Zanasi, R.; *Chem. Phys. Lett.* (1990), 165, 79.
28. Simons, J.; *J. Phys. Chem.* (1991), 95, 1017.
29. László, I.; Udvardi, L.; *Chem. Phys. Lett.* (1987), 136, 418.
30. Larsson, S.; Volosov, A.; Rosén, A.; *Chem. Phys. Lett.* (1987), 137, 501.

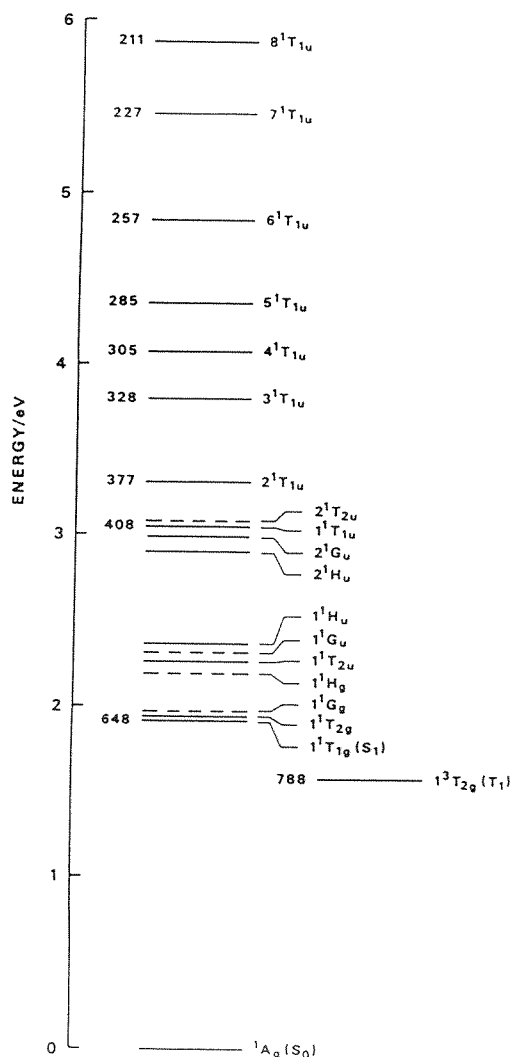


Figure 6. Probable ordering of the low lying states of  $C_{60}$ . Only the lowest triplet is shown. Above  $2T_{2u}$ , only  $T_{1u}$  states are shown. Approximate 0-0 wavelengths (in nm) are indicated at the left of some states.